inorganics

MDPI

Article

Crystal Structures of DNA Intercalating Agents Dipyrido[3,2-f:2′,3′-h]quinoxaline (dpq), (Benzo[*i*]dipyrido[3,2-a:2′,3′c]phenazine (dppn), and [Ir(ppy)$_2$(dppn)][PF$_6$] (Where Hppy = 2-Phenylpyridine)

Marisa James [1], Madelyn R. Shevlin [1], Thomas B. Green [1], Megan M. Smart [2], Colin D. McMillen [2,*] and Jared A. Pienkos [1,*]

[1] Department of Chemistry & Physics, The University of Tennessee at Chattanooga, Chattanooga, TN 37403, USA
[2] Department of Chemistry, Clemson University, Clemson, SC 29634, USA
* Correspondence: cmcmill@clemson.edu (C.D.M.); jared-pienkos@utc.edu (J.A.P.)

Abstract: Pyrazino-phenanthroline ligands are commonly used with transition metals as DNA intercalation agents. Herein, we report the characterization of two commonly utilized pyrazino-phenanthroline ligands, dipyrido[3,2-f:2′,3′-h]quinoxaline (dpq) and (benzo[*i*]dipyrido[3,2-a:2′,3′c]phenazine (dppn), by single-crystal X-ray diffraction. Additionally, the characterization of [Ir(ppy)$_2$(dppn)][PF$_6$], where Hppy = 2-phenylpyridine, by single-crystal X-ray diffraction is described. Both the dpq and dppn ligands crystallize as chloroform solvates where the chloroform molecule occupies the equivalent binding pocket of a metal in metal complexes of these ligands. These pyrazino-phenanthrolines are largely planar, with the dppn ligand displaying a slight twist. When the dppn ligand is coordinated to iridium(III), the dppn ligand on the resulting complex displays a significant degree of bending along the longitudinal direction of the ligand. This iridium (III) complex crystallizes as a CH_2Cl_2 and Et_2O solvate and due to the volatility of these solvents these crystals are only stable for a few seconds outside of the mother liquor. The structures of the free ligands and the [Ir(ppy)$_2$(dppn)][PF$_6$] complex all display extensive π stacking interactions.

Keywords: pyrazino-phenanthroline; dpq; dppn; intercalation; iridium (III) complex

Citation: James, M.; Shevlin, M.R.; Green, T.B.; Smart, M.M.; McMillen, C.D.; Pienkos, J.A. Crystal Structures of DNA Intercalating Agents Dipyrido[3,2-f:2′,3′-h]quinoxaline (dpq), (Benzo[*i*]dipyrido[3,2-a:2′,3′c]phenazine (dppn), and [Ir(ppy)$_2$(dppn)][PF$_6$] (Where Hppy = 2-Phenylpyridine). *Inorganics* **2023**, *11*, 353. https://doi.org/10.3390/inorganics11090353

Academic Editor: László Kótai

Received: 31 July 2023
Revised: 23 August 2023
Accepted: 25 August 2023
Published: 29 August 2023

1. Introduction

Polypyridyl ligands with extended conjugation have gained interest as DNA intercalation agents because of their planar structures [1]. One class of these molecules, the pyrazino-phenanthroline ligands, are commonly used intercalation agents that can be synthesized by a condensation reaction with 1,10-phenanthrolene-5,6-dione and an appropriate diamine (Scheme 1) [2–4]. Exploiting diamines with aromatic backbones can result in pyrazino-phenanthroline derivatives with more extended conjugation, which are commonly used in combination with transition metal compounds to provide species that can interact with DNA. Because DNA is negatively charged, cationic metal complexes are commonly utilized for advantageous electrostatic interactions [5].

For example, [Ru(bpy)$_2$(dppz)]$^{2+}$ serves as a luminescent DNA probe (Scheme 2) [6]. In aqueous environments, this compound's luminescence is quenched by H_2O through a proton transfer to the pyrazine moieties. Once [Ru(bpy)$_2$(dppz)]$^{2+}$ is intercalated into DNA, the compound lumineses as H_2O is no longer able to quench this process. In addition to Ru(II) derivatives [7–11], other metal centers (e.g., Ir(III) [12], Os(II) [13], Re(I) [14–16], Rh(III) [17], Cr(III) [18], Co(III) [19], and Ni(II) [19]) with similar ligand structures have been exploited for their DNA binding properties. For example, Lo et al. demonstrated that the Ir(III) species [Ir(ppy)$_2$(dppn)][PF$_6$](where Hppy = 2-phenylpyridine) intercalates DNA (Scheme 2), which was determined through absorption and emission titration experiments [12].

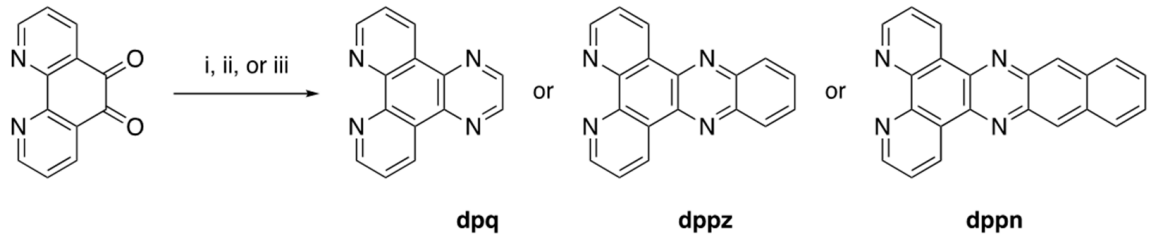

Scheme 1. Synthesis of the dipyrido[3,2-f:2′,3′-h]quinoxaline (dpq), dipyrido[3,2-a:2′,3′-c]phenazine (dppz), and (benzo[*i*]dipyrido[3,2-a:2′,3′c]phenazine (dppn). Conditions i = ethylenediamine, ii = o-phenylenediamine, iii = 2,3-diaminonaphthalene.

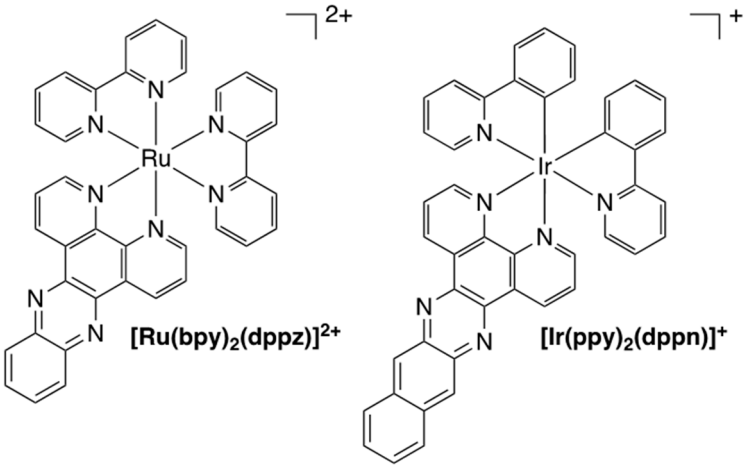

Scheme 2. Schematics of $[Ru(bpy)_2(dppn)]^{2+}$ and $[Ir(ppy)_2(dppn)]^{+}$ that are shown to participate in DNA intercalation.

Although the utility of dpq, dppz, and dppn as coordinating ligands in metal complexes has been described in the literature, in terms of the free ligands, only the crystal structure of the dppz ligand has been so far reported, as a $CHCl_3$ [20] and MeOH solvate [21]. Herein, we present the crystal structure of the dpq and dppn ligands as chloroform solvates to provide comparative structures of these useful ligands in their non-coordinated form. We also synthesized the previously reported $[Ir(ppy)_2(dppn)][PF_6]$organometallic compound, for which no structure was previously reported [12], and determined its crystal structure as an Et_2O and CH_2Cl_2 solvate.

2. Results and Discussion

2.1. Synthesis

The two investigated pyrazino-phenanthroline ligands were synthesized by heating the appropriate diamine in the presence of 1,10-phenanthroline-5,6-dione followed by solvent washings or recrystallization. Characterization by ^1H NMR spectroscopy was utilized to confirm the purity of each species. The dpq ligand displayed four ^1H resonances at 9.6, 9.4, 9.1, and 7.9 ppm and the dppn ligand displayed six ^1H resonances at 9.6, 9.3, 8.9, 8.2, 7.8, and 7.6 ppm, which matched previously reported characterization (Supplementary Materials, Figures S1 and S2).

The Ir(III) species, $[Ir(ppy)_2(dppn)][PF_6]$, was synthesized by heating a chloro-bridged iridium dimer, $[Ir(ppy)_2(\mu\text{-}Cl)]_2$, in the presence of dppn and ethylene glycol. Upon addition of a saturated aqueous solution of NH_4PF_6, a precipitate formed that was collected and washed with H_2O and Et_2O to give $[Ir(ppy)_2(dppn)][PF_6]$. Characterization by ^1H NMR spectroscopy was utilized to confirm the purity of this species, which matched the previously reported data (Supplementary Materials, Figure S3) [12].

2.2. Crystal Structure of dpq·$CHCl_3$

The free dpq ligand crystallized as the chloroform solvate, dpq·$CHCl_3$, in the monoclinic space group $P2_1/c$, with Z = 4. The asymmetric unit consists of one unique molecule each of dpq and $CHCl_3$ (Figure 1a). The dpq molecule is planar, as indicated by the following key dihedral angles about the central benzene ring: N1-C5-C6-N2 = −1.0 (4)°, C9-C10-C11-N4 = 2.4 (4)°, and C3-C4-C12-N3 = −0.9 (4)°. These are of similar magnitude to the dihedral angles in the unbound dpq ligands that are cocrystallized in the structure of the bis(dihydrogen bis(pyrazolyl)borate-N,N′)-(pyrazino[2,3-f][1,10]phenanthroline-iron complex [22]. Planarity is also generally maintained among the numerous examples of dpq ligands that are coordinated to transition metals or lanthanide ions [20,22–25].

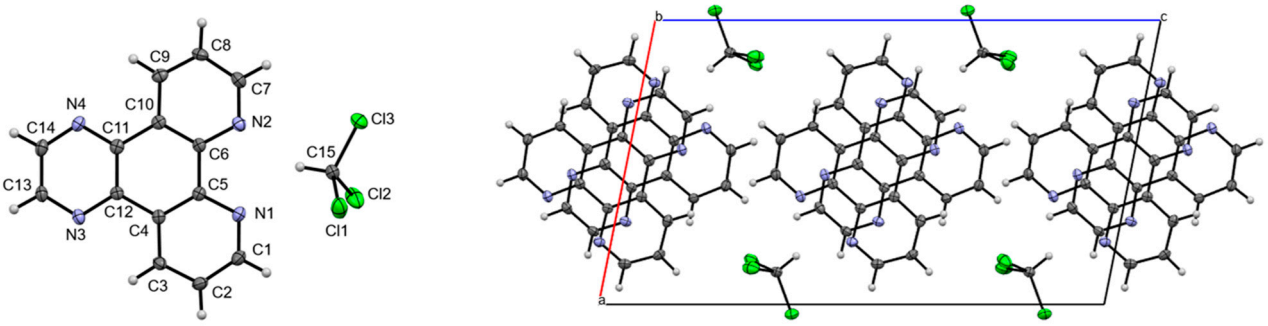

(**a**) (**b**)

Figure 1. Crystal structure of dpq·$CHCl_3$: (**a**) Molecular structure shown as 50% probability ellipsoids; (**b**) Packing diagram viewed along the *b*-axis showing the offset nature of the stacked dpq molecules.

Neighboring dpq molecules form offset stacks along the *b*-axis (Figures 1b and 2a), having a parallel plane-to-plane distance of 3.213 Å, supporting π···π interactions. The $CHCl_3$ molecules provide important connectivity to form chains of alternating $CHCl_3$ and dpq molecules propagating along the *a*-axis (Figure 2b). The hydrogen atom of the $CHCl_3$ molecule forms bifurcated C-H···N interactions with the pyridyl nitrogen atoms (N1, N2) of one dpq molecule (H···N = 2.34 Å and 2.30 Å), while the Cl3 atom forms a Cl···N halogen bonding interaction (3.127 (3) Å) to the N3 atom of the pyrazine ring of a second dpq molecule. Through the bifurcated C-H···N interactions, the $CHCl_3$ molecule occupies a similar binding pocket to transition metals that coordinate dpq.

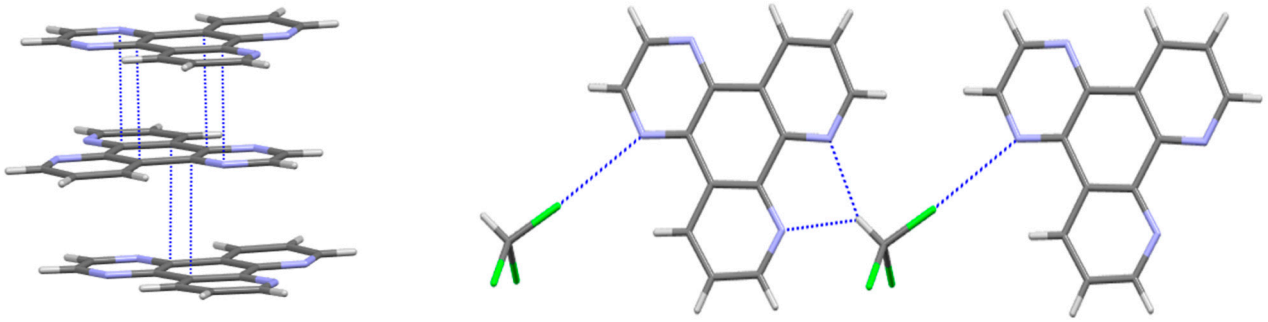

(**a**) (**b**)

Figure 2. Intermolecular interactions in dpq·$CHCl_3$: (**a**) Parallel stacked dpq molecules; (**b**) Chain formation facilitated by the $CHCl_3$ solvent molecules through C-H···N and Cl···N interactions.

2.3. Crystal Structure of dppn·$CHCl_3$

The free dppn ligand also crystallized as the chloroform solvate, dppn·$CHCl_3$, in the orthorhombic space group *Pbca*, with Z = 8. The asymmetric unit consists of one unique

molecule each of dppn and $CHCl_3$ (Figure 3a). Dihedral angles about the central benzene ring again indicate a largely planar molecule with a very slight twist (N1-C5-C10-N2 = −1.7 (2)°, C3-C4-C11-N3 = −1.1 (2)°, and C8-C9-C12-N4 = 5.2 (2)°). Similar twists up to about 7° have been observed in dppn ligands coordinated to metal centers [20,26–35].

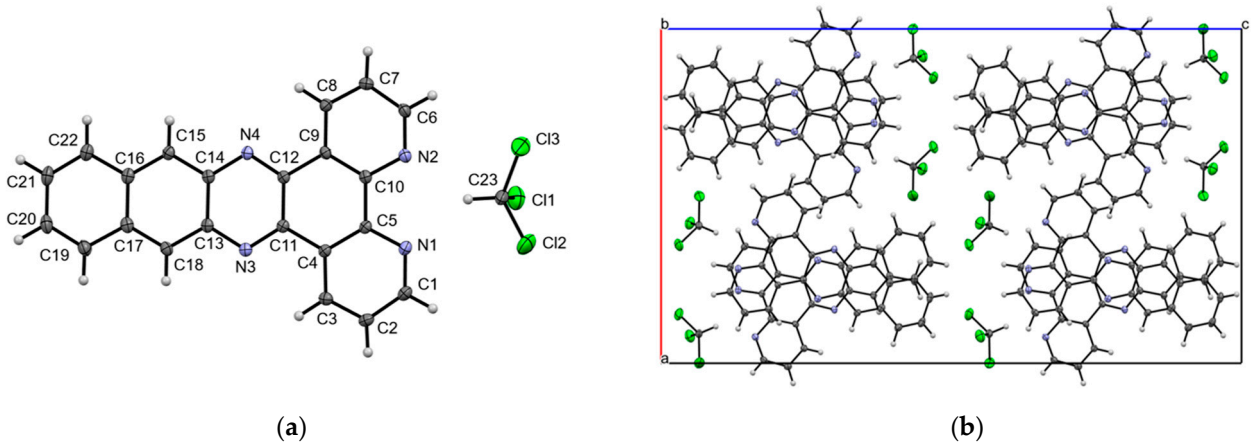

(**a**) (**b**)

Figure 3. Crystal structure of dppn·$CHCl_3$: (**a**) Molecular structure shown as 50% probability ellipsoids; (**b**) Packing diagram viewed along the *b*-axis showing the offset nature of the stacked dppn molecules.

Neighboring molecules stack in slightly off-parallel fashion (Figures 3b and 4a), with their neighboring mean planes inclined at 8.7(3)° to one another. The stacking occurs approximately along the [1 28 2] direction, and the average distance between planes stacked in that direction is 3.305 Å. Similar to the dpq solvate, the $CHCl_3$ molecule maintains bifurcated C-H···N interactions to the pyridyl nitrogen atoms (H···N = 2.36 Å and 2.27 Å), also occupying a similar binding pocket to metal ions in dppn complexes. However, the chlorine atoms in dppn·$CHCl_3$ do not participate in any halogen bonding interactions as they do in dpq·$CHCl_3$. Instead, chains of dppn molecules are formed through C-H···N interactions to the N3 atom of the pyrazine ring (H···N = 2.66 Å). These chains propagate along the *a*-axis (Figure 4b).

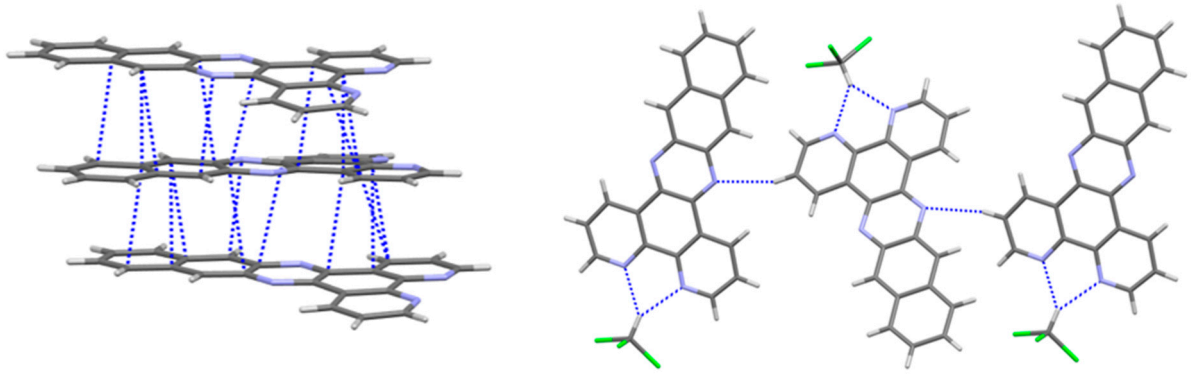

(**a**) (**b**)

Figure 4. Intermolecular interactions in dppn·$CHCl_3$: (**a**) Slightly off-parallel stacked dppn molecules; (**b**) Chain formation facilitated by C-H···N interactions of neighboring dppn molecules.

2.4. Crystal Structure of [Ir(ppy)$_2$(dppn)][PF$_6$] · 0.875 CH$_2$Cl$_2$, 0.25 C$_4$H$_{10}$O

The iridium(III) complex of dppn and 2-phenylpyridine (Hppy) (Figure 5a) was prepared as the $[PF_6]^-$ salt and crystallized as a complex solvate involving disordered CH_2Cl_2 and $C_4H_{10}O$ molecules, $[Ir(ppy)_2(dppn)][PF_6] \cdot 0.875\ CH_2Cl_2, 0.25\ C_4H_{10}O$. The complex crystallizes in the triclinic space group *P*-1 with Z = 4, and two unique cationic complexes and two unique $[PF_6]^-$ anions in the asymmetric unit, as well as the disordered solvent

molecules as described in Section 3 below (Figure 5b). In $[Ir(ppy)_2(dppn)][PF_6]$, the iridium(III) center is six-coordinate, with the ppy ligands each coordinating through one carbon and one nitrogen atom, and the dppn ligand coordinating through both of the pyridyl nitrogen atoms. The Ir-N bonds to dppn are oriented opposite the Ir-C bonds to ppy, leading to a measurable *trans*-effect elongating the Ir-N bonds to dppn (2.122 (9) Å to 2.184 (9) Å) compared to the Ir-N bonds to ppy (2.041 (9) Å to 2.065 (9) Å). This is similar to what is observed in the structures of $[Ir(ppy)_2(dppz)][PF_6]$ [12] and $[Ir(F_2ppy)_2(dpq)][PF_6]$ [24] which have a similar coordination patterns, Ir-N distances, and *trans*-effects. Likewise, the Ir-C bond lengths of $[Ir(ppy)_2(dppn)][PF_6]$ (1.993 (11) Å to 2.033 (12) Å) are in good agreement with those complexes.

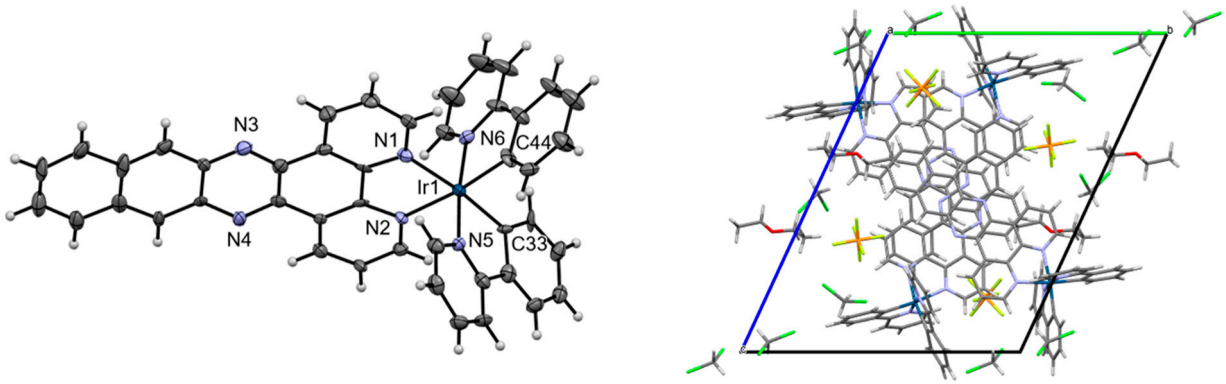

(**a**) (**b**)

Figure 5. Crystal structure of $[Ir(ppy)_2(dppn)][PF_6] \cdot 0.875\ CH_2Cl_2$, $0.25\ C_4H_{10}O$: (**a**) Molecular structure of one of the unique complexes, shown as 50% probability ellipsoids; (**b**) Packing diagram viewed along the *a*-axis showing complexes stacking from offset overlap of their dppn ligands, with anions and solvent molecules assembling around the stacked complexes.

The coordinated dppn ligands in the two unique $[Ir(ppy)_2(dppn)]^+$ complexes of $[Ir(ppy)_2(dppn)][PF_6]$ exhibit similar C-C-C-N dihedral angles (up to 5.2 (17)°) to those in $dppn{\cdot}CHCl_3$, but rather than producing a slightly twisted effect along the longitudinal direction of the fused ring system, in $[Ir(ppy)_2(dppn)][PF_6]$, the torsion leads to a meaningful flexible or bending effect. For example, using the N-C-C-N binding pocket formed by the pyridyl rings as a reference plane, the last carbon atoms of the longitudinal fused ring system depart from this plane by 0.35 Å and 0.41 Å in the unique Ir1 complex, and 1.88 Å and 1.95 Å in the unique Ir2 complex (Figure 6).

Figure 6. Flexibility of the coordinated dppn ligand in the $[Ir(ppy)_2(dppn)][PF_6]$ complex in $[Ir(ppy)_2(dppn)][PF_6] \cdot 0.875\ CH_2Cl_2$, $0.25\ C_4H_{10}O$.

The complexes assemble in stacks along the *a*-axis via offset overlap of the dppn ligands on neighboring complexes (Figure 7). In this way, the average stacking distance between dppn ligands is 3.133 Å. The stacking interactions are complemented by C-H···π interactions between the dppn ligand of one complex and the ppy ligand of the next complex along the stack. Additional C-H···π interactions between the ppy ligands of complexes in neighboring stacks along the *b*-axis and *c*-axis create a three-dimensional network. The network is then reinforced by C-H···F interactions between the cationic complexes and the $[PF_6]^-$ anions. The CH_2Cl_2 and Et_2O solvent molecules fill the remaining space in the lattice. Due to the volatility of these solvents and the significant void space between complexes, crystals of $[Ir(ppy)_2(dppn)][PF_6] \cdot 0.875\ CH_2Cl_2, 0.25\ C_4H_{10}O$ are only stable outside of the mother liquor for a few seconds.

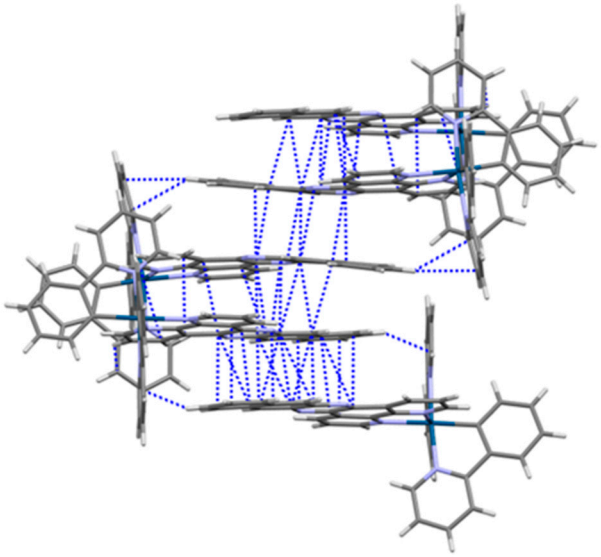

Figure 7. A stack of the $[Ir(ppy)_2(dppn)][PF_6]$ complex supported by offset overlap of dppn ligands and C-H···π interactions in $[Ir(ppy)_2(dppn)][PF_6] \cdot 0.875\ CH_2Cl_2, 0.25\ C_4H_{10}O$.

The potential for $[Ir(ppy)_2(dppn)][PF_6]$ to intercalate into DNA may be understood in the context of the elegant structure determinations of cocrystals of Ru complexes of dppz with oligonucleotide sequences. In one study, the Λ-$[Ru(TAP)_2(dppz)]^{2+}$ complex (TAP = 1,4,5,8-tetraazaphenanthrene) cocrystallizes with the d(TCGGCGCCGA) sequence via intercalation of the dppz ligand and semiintercalation of the TAP ligands to produce a non-covalently cross-linked and kinked structure [36]. In that structure, the dppz ligand exhibits stacking interactions between its pyrazine ring and purine rings, while showing no interactions with solvated water molecules [36]. In another study, a Δ-$[Ru(bpy)_2(dppz)]^{2+}$ complex interacts with the mismatched $d(CGGAAATTACCG)_2$ sequence via metalloinsertion and ejection of mismatched adenosines, metallointercalation, and end-capping [37]. In that study, various dppz intercalation depths are noted, involving the central and distal rings of the ligand [37]. The propensity of stacking interactions observed in the structure of $[Ir(ppy)_2(dppn)][PF_6]$ (and for that matter, the free dpq or dppn ligands) in the present study suggests it has similar potential as a versatile intercalation complex. The similarity of the ppy ligands to TAP and bpy ligands in the cocrystallized compounds may also suggest that the ancillary ligand interactions that are prevalent and influential in the structures reported in [36,37] may also be operable for $[Ir(ppy)_2(dppn)][PF_6]$.

3. Materials and Methods

3.1. Reagents and General Procedures

All reagents were purchased from Acros Organics (ethylenediamine), Alfa Aesar ($IrCl_3 \cdot H_2O$), Ambeed (1,10-phenanthroline-5,6-dione), Fisher Scientific (CH_3OH), Oakwood Chemicals (2,3-diaminonaphthalene), TCI Chemicals (2-phenylpyridine), and VWR

(CH_3CH_2OH) and used as received. $[Ir(ppy)_2(\mu\text{-}Cl)]_2$ was synthesized according to a reported literature procedure [38]. All reactions were performed under a N_2 atmosphere. NMR samples were prepared by dissolving ~10 mg of sample in the appropriate deuterated solvent. The ^{1}H-NMR spectra were recorded on a Jeol-400 MHz spectrometer. The ^{1}H-NMR chemical shifts are referenced to residual protons in the deuterated solvent. Elemental analysis was performed by Atlantic Microlab (Norcross, GA, USA).

3.2. Synthesis of dpq (Adapted from the Literature [3])

1,10-phenanthroline-5,6-dione (0.5 g, 2.381 mmol) and ethylenediamine (0.223 mL, 3.341 mmol) were heated in CH_3CH_2OH (175 mL) at 40 °C for 3 h, before stirring at room temperature for 17 h. The solvent was then removed under vacuum to afford a cream-colored product. The product was purified by recrystallization using CH_3OH to yield 0.7521 g, 97% yield) a cream colored solid. Crystals were grown at room temperature using vapor-vapor diffusion in $CHCl_3/Et_2O$. Elemental Analysis for $C_{14}H_8N_4$: Calculated (%): C, 72.40; H, 3.47; N, 24.12. Found (%): C, 72.11; H, 3.41; N, 24.32.

3.3. Synthesis of dppn (Adapted from the Literature [2])

1,10-phenanthroline-5,6-dione (0.4967 g, 2.365 mmol) and 2,3-diaminonaphthalene (0.4101 g, 2.596 mmol) were refluxed in CH_3OH (75 mL). After 1 h, the bright orange precipitate that formed was filtered and washed with 25 mL each of H_2O, CH_3OH, and Et_2O. The product (0.3489 g, 45% yield) was obtained as an orange solid. Crystals were grown at room temperature using vapor-vapor diffusion in $CHCl_3$/Hexanes. Elemental Analysis for $C_{22}H_{12}N_4 \cdot 1.5\ H_2O$: Calculated (%): C, 73.53; H, 4.21; N, 15.59. Found (%): C, 73.88; H, 4.00; N, 15.83.

3.4. Synthesis of $[Ir(ppy)_2(dppn)][PF_6]$ (Adapted from the Literature [12])

Ethylene glycol (5 mL) was added to $[Ir(ppy)_2(\mu\text{-}Cl)]_2$ (0.1011g, 0.0944 mmol) and dppn (0.0677g, 0.2037 mmol) and the resulting mixture was heated at 150 °C under nitrogen. After 16 h, a saturated solution of NH_4PF_6 (4.575 g, 28.07 mmol) in H_2O (10 mL) was added to the bright orange reaction mixture before performing a filtration with sequential washings of H_2O (3 × 10 mL) and Et_2O (3 × 10 mL). The product was obtained as an orange solid (0.181 g, 91% yield) and crystals were grown at room temperature using vapor-vapor diffusion in CH_2Cl_2/Et_2O. Elemental Analysis for $C_{44}H_{28}F_6IrN_6P \cdot 2\ H_2O$: Calculated (%): C, 52.12; H, 3.18; N, 8.29. Found (%): C, 51.94; H, 2.97; N, 8.41.

3.5. X-ray Crystallography

Single crystal X-ray diffraction data were collected at 100 K using a Bruker D8 Venture diffractometer with Mo Kα radiation (λ = 0.71073 Å) from a microfocus source, and a Photon 2 detector. Data were collected using 0.5° oscillations of φ and ω. Data were integrated, scaled, and corrected for absorption (multi-scan) using SAINT and SADABS programs within the Apex 3 software suite. The initial structural model was determined by intrinsic phasing using SHELXT [39], and subsequently refined by full-matrix least squares techniques on F^2 using SHELXL [40]. All non-hydrogen atoms were refined anisotropically. Hydrogen atoms attached to carbon atoms were refined in calculated positions using appropriate riding models. The $CHCl_3$ solvent molecules cocrystallized in the structures of dpq·$CHCl_3$ and dppn·$CHCl_3$ were found to be fully occupied and well ordered. The solvent contribution to the structure of $[Ir(ppy)_2(dppn)][PF_6]$ consisted of one fully occupied, well-ordered CH_2Cl_2 molecule, three quarter-occupied CH_2Cl_2 molecules, and one half-occupied Et_2O molecule, in addition to the two unique iridium complexes and $[PF_6]^-$ counterions, leading to a composition of $[Ir(ppy)_2(dppn)][PF_6] \cdot 0.875\ CH_2Cl_2, 0.25\ C_4H_{10}O$. Due to the presence of these highly volatile solvent molecules in the crystalline lattice, the crystals were mounted under cold flowing nitrogen, and had to be immediately quenched to 100 K on the diffractometer. Without immediate quenching to 100 K the crystals decomposed after about 8–10 s, even under paratone oil. Crystallographic data are given in Table 1.

CSD 2285801-2285803 contain the supplementary crystallographic data for this paper. These data can be obtained free of charge via http://www.ccdc.cam.ac.uk/conts/retrieving.html (accessed on 30 July 2023) (or from the CCDC, 12 Union Road, Cambridge CB2 1EZ, UK; Fax: +44 1223 336033; E-mail: deposit@ccdc.cam.ac.uk).

Table 1. Crystallographic data.

	dpq·CHCl$_3$	**dppn·CHCl$_3$**	**[Ir(ppy)$_2$(dppn)][PF$_6$] · 0.875 CH$_2$Cl$_2$, 0.25 C$_4$H$_{10}$O**
Formula	$C_{15}H_9Cl_3N_4$	$C_{23}H_{13}Cl_3N_4$	$C_{45.88}H_{32.25}Cl_{1.75}F_6IrN_6O_{0.25}P$
F. W. (g/mol)	351.61	451.72	1070.73
Temperature (K)	100 (2)	100 (2)	100 (2)
Crystal System	Monoclinic	Orthorhombic	Triclinic
Space group	$P2_1/c$ (no. 14)	*Pbca* (no. 61)	*P*-1 (no. 2)
a (Å)	11.3166 (7)	18.1564 (5)	12.5328 (8)
b (Å)	6.6154 (4)	6.93200 (10)	18.0553 (11)
c (Å)	19.8106 (12)	31.6298 (7)	22.0638 (15)
α (°)	90	90	112.989 (2)
β (°)	101.289 (2)	90	93.685 (2)
γ (°)	90	90	103.869 (2)
Volume (Å^3)	1454.40 (15)	3980.93 (15)	4392.0 (5)
Z	4	8	4
D (calcd) (mg/m^3)	1.606	1.507	1.619
μ, mm^{-1}	0.630	0.479	3.249
F (000)	712	1840	2109
Cryst. Size (mm)	0.02 × 0.03 × 0.11	0.09 × 0.10 × 0.41	0.02 × 0.08 × 0.23
θ range, °	3.05 to 25.74	2.58 to 28.42	1.81 to 25.80
Reflns. collected	39,390	37,847	85,424
Indep. Reflns.	2758	4971	16,732
No. of parameters	199	271	1198
R indices (I > 2σ(I))	R_1 = 0.0412 [a] wR_2 = 0.0879 [b]	R_1 = 0.0378 [a] wR_2 = 0.0895 [b]	R_1 = 0.0719 [a] wR_2 = 0.1849 [b]
R indices (all data)	R_1 = 0.0725 [a] wR_2 = 0.1047 [b]	R_1 = 0.0533 [a] wR_2 = 0.0986 [b]	R_1 = 0.0968 [a] wR_2 = 0.2022 [b]
S	1.034	1.022	1.105

[a] $R_1 = \Sigma||F_o| - |F_c||/\Sigma|F_o|$. [b] $wR_2 = \{\Sigma[w(F_o^2 - F_c^2)^2]/\Sigma[wF_o^2]^2\}^{1/2}$.

4. Conclusions

We were able to characterize the commonly utilized intercalating agents dpq and dppn by single-crystal X-ray diffraction. While these and similarly structured pyrazino-phenanthroline ligands are often exploited to generate transition metal intercalating agents [5–19], only the crystal structure of the dppz ligand has been previously reported [20,21]. Establishing the structures of the free ligands provides useful benchmarks for their metal coordination structural chemistry. The crystal structure of the dpq and dppn ligands indicate that these species are largely planar, with the dppn ligand displaying a slight twist. Upon coordination to iridium, as [Ir(ppy)$_2$(dppn)][PF$_6$], the dppn ligand exhibits longitudinal bending, as determined by single-crystal X-ray diffraction of this iridium(III) species.

Supplementary Materials: The following supporting information can be downloaded at: https://www.mdpi.com/article/10.3390/inorganics11090353/s1, Figure S1: ^{1}H NMR of dipyrido[3,2-f:2′,3′-h]quinoxaline (dpq) in CDCl$_3$; Figure S2: ^{1}H NMR of benzo[*i*]dipyrido[3,2-a:2′,3′c]phenazine (dppn) in CDCl$_3$; Figure S3: ^{1}H NMR [Ir(ppy)$_2$(dppn)][PF$_6$] in (CD$_3$)$_2$CO.

Author Contributions: M.J.: Investigation, Formal analysis, Data curation, Writing—reviewing and editing. M.R.S.: Investigation, Data curation. T.B.G.: Investigation, Data Curation. M.M.S.: Investigation, Data Curation. C.D.M.: Investigation, Formal analysis, Data curation, Writing—original draft. J.A.P.: Conceptualization, Writing—original draft, Methodology, Supervision, Project administration. All authors have read and agreed to the published version of the manuscript.

Funding: This research was funded by the Grote Research Fund at the University of Tennessee at Chattanooga.

Data Availability Statement: CSD 2285801-2285803 contain the supplementary crystallographic data for this paper. These data can be obtained free of charge via http://www.ccdc.cam.ac.uk/conts/retrieving.html (accessed on 30 July 2023) (or from the CCDC, 12 Union Road, Cambridge CB2 1EZ, UK; Fax: +44 1223 336033; E-mail: deposit@ccdc.cam.ac.uk).

Conflicts of Interest: The authors declare no conflict of interest.

References

1. Georgiades, S.N.; Vilar, R. Interaction of metal complexes with nucleic acids. *Annu. Rep. Sect. A (Inorg. Chem.)* **2010**, *106*, 481–503. [CrossRef]
2. Foxon, S.P.; Green, C.; Walker, M.G.; Wragg, A.; Adams, H.; Weinstein, J.A.; Parker, S.C.; Meijer, A.J.H.M.; Thomas, J.A. Synthesis, Characterization, and DNA Binding Properties of Ruthenium(II) Complexes Containing the Redox Active Ligand Benzo[*i*]dipyrido[3,2-a:2′,3′-c]phenazine-11,16-quinone. *Inorg. Chem.* **2012**, *51*, 463–471. [CrossRef]
3. Deshpande, M.S.; Kumbhar, A.S.; Näther, C. Stabilization of acyclic water tetramer in a copper(ii) malonate framework structure. *Dalton Trans.* **2010**, *39*, 9146–9152. [CrossRef] [PubMed]
4. Nagaraj, K.; Senthil Murugan, K.; Thangamuniyandi, P.; Sakthinathan, S. Synthesis, Micellization Behaviour, DNA/RNA Binding and Biological Studies of a Surfactant Cobalt(III) Complex With Dipyrido[3,2-a:2′,4′-c](6,7,8,9-tetrahydro)phenazine. *J. Fluoresc.* **2014**, *24*, 1701–1714. [CrossRef] [PubMed]
5. Di Pietro, M.L.; La Ganga, G.; Nastasi, F.; Puntoriero, F. Ru(II)-Dppz Derivatives and Their Interactions with DNA: Thirty Years and Counting. *Appl. Sci.* **2021**, *11*, 3038. [CrossRef]
6. Friedman, A.E.; Chambron, J.C.; Sauvage, J.P.; Turro, N.J.; Barton, J.K. A molecular light switch for DNA: $Ru(bpy)_2(dppz)^{2+}$. *J. Am. Chem. Soc.* **1990**, *112*, 4960–4962. [CrossRef]
7. Greguric, I.; Aldrich-Wright, J.R.; Collins, J.G. A 1H NMR Study of the Binding of Δ-$[Ru(phen)_2DPQ]^{2+}$ to the Hexanucleotide $d(GTCGAC)_2$. Evidence for Intercalation from the Minor Groove. *J. Am. Chem. Soc.* **1997**, *119*, 3621–3622. [CrossRef]
8. Collins, J.G.; Sleeman, A.D.; Aldrich-Wright, J.R.; Greguric, I.; Hambley, T.W. A 1H NMR Study of the DNA Binding of Ruthenium(II) Polypyridyl Complexes. *Inorg. Chem.* **1998**, *37*, 3133–3141. [CrossRef]
9. Collins, J.G.; Aldrich-Wright, J.R.; Greguric, I.D.; Pellegrini, P.A. Binding of the Δ- and Λ-Enantiomers of $[Ru(dmphen)_2dpq]^{2+}$ to the Hexanucleotide $d(GTCGAC)_2$. *Inorg. Chem.* **1999**, *38*, 5502–5509. [CrossRef]
10. O'Donoghue, K.A.; Kelly, J.M.; Kruger, P.E. Unusual photophysical switching in a Ru(ii) diimine DNA probe caused by amide functionalisation. *Dalton Trans.* **2004**, *2004*, 13–15. [CrossRef]
11. O'Donoghue, K.; Penedo, J.C.; Kelly, J.M.; Kruger, P.E. Photophysical study of a family of $[Ru(phen)_2(Medpq)]^{2+}$ complexes in different solvents and DNA: A specific water effect promoted by methyl substitution. *Dalton Trans.* **2005**, *2005*, 1123–1128. [CrossRef] [PubMed]
12. Lo, K.K.-W.; Chung, C.-K.; Zhu, N. Nucleic Acid Intercalators and Avidin Probes Derived from Luminescent Cyclometalated Iridium(III)–Dipyridoquinoxaline and –Dipyridophenazine Complexes. *Chem. Eur. J.* **2006**, *12*, 1500–1512. [CrossRef] [PubMed]
13. Holmlin, R.E.; Yao, J.A.; Barton, J.K. Dipyridophenazine Complexes of Os(II) as Red-Emitting DNA Probes: Synthesis, Characterization, and Photophysical Properties. *Inorg. Chem.* **1999**, *38*, 174–189. [CrossRef]
14. Stoeffler, H.D.; Thornton, N.B.; Temkin, S.L.; Schanze, K.S. Unusual Photophysics of a Rhenium(I) Dipyridophenazine Complex in Homogeneous Solution and Bound to DNA. *J. Am. Chem. Soc.* **1995**, *117*, 7119–7128. [CrossRef]
15. Metcalfe, C.; Webb, M.; Thomas, J.A. A facile synthetic route to bimetallic ReI complexes containing two dppz DNA intercalating ligands. *Chem. Commun.* **2002**, *2002*, 2026–2027. [CrossRef]
16. Lo, K.K.-W.; Tsang, K.H.-K. Bifunctional Luminescent Rhenium(I) Complexes Containing an Extended Planar Diimine Ligand and a Biotin Moiety. *Organometallics* **2004**, *23*, 3062–3070. [CrossRef]
17. Herebian, D.; Sheldrick, W.S. Synthesis and DNA binding properties of bioorganometallic (η5-pentamethylcyclopentadienyl)iridium(iii) complexes of the type $[(\eta5\text{-}C5Me5)Ir(Aa)(dppz)]^+$ (dppz = dipyrido[3,2-a:2′,3′-c]phenazine, n = 1–3), with S-coordinated amino acids (Aa) or peptides. *J. Chem. Soc. Dalton Trans.* **2002**, *2002*, 966–974. [CrossRef]
18. Barker, K.D.; Benoit, B.R.; Bordelon, J.A.; Davis, R.J.; Delmas, A.S.; Mytykh, O.V.; Petty, J.T.; Wheeler, J.F.; Kane-Maguire, N.A.P. Intercalative binding and photoredox behavior of $[Cr(phen)_2(dppz)]^{3+}$ with B-DNA. *Inorg. Chim. Acta* **2001**, *322*, 74–78. [CrossRef]
19. Arounaguiri, S.; Maiya, B.G. Dipyridophenazine Complexes of Cobalt(III) and Nickel(II): DNA-Binding and Photocleavage Studies. *Inorg. Chem.* **1996**, *35*, 4267–4270. [CrossRef] [PubMed]
20. Kulmaczewski, R.; Shepherd, H.J.; Cespedes, O.; Halcrow, M.A. A Homologous Series of $[Fe(H_2Bpz_2)_2(L)]$ Spin-Crossover Complexes with Annelated Bipyridyl Co-Ligands. *Inorg. Chem.* **2014**, *53*, 9809–9817. [CrossRef]
21. Phillips, T.; Haq, I.; Meijer, A.J.H.M.; Adams, H.; Soutar, I.; Swanson, L.; Sykes, M.J.; Thomas, J.A. DNA Binding of an Organic dppz-Based Intercalator. *Biochemistry* **2004**, *43*, 13657–13665. [CrossRef]
22. Zhernakov, M.A.; Sedykh, A.E.; Becker, J.; Maxeiner, M.; Müller-Buschbaum, K.; Shtyrlin, V.G. Three ytterbium(III) complexes with aromatic N-donors: Synthesis, structure, photophysical properties and thermal stability. *Z. Für Anorg. Und Allg. Chem.* **2022**, *648*, e202200230. [CrossRef]
23. Zhang, C.; Ma, X.; Cen, P.; Yang, H.; He, Z.; Guo, Y.; Tian, D.; Liu, X. Dual-sensitized Eu(III)/Tb(III) complexes exhibiting tunable luminescence emission and their application in cellular-imaging. *Dalton Trans.* **2022**, *51*, 3180–3187. [CrossRef] [PubMed]

24. Gonzalez, I.; Dreyse, P.; Cortes-Arriagada, D.; Sundararajan, M.; Morgado, C.; Brito, I.; Roldan-Carmona, C.; Bolink, H.J.; Loeb, B. A comparative study of Ir(III) complexes with pyrazino[2,3-f][1,10]phenanthroline and pyrazino[2,3-f][4,7]phenanthroline ligands in light-emitting electrochemical cells (LECs). *Dalton Trans.* **2015**, *44*, 14771–14781. [CrossRef]
25. Sarkar, T.; Kumar, A.; Sahoo, S.; Hussain, A. Mixed-Ligand Cobalt(III) Complexes of a Naturally Occurring Coumarin and Phenanthroline Bases as Mitochondria-Targeted Dual-Purpose Photochemotherapeutics. *Inorg. Chem.* **2021**, *60*, 6649–6662. [CrossRef]
26. Travis, W.; Knapp, C.E.; Savory, C.N.; Ganose, A.M.; Kafourou, P.; Song, X.; Sharif, Z.; Cockcroft, J.K.; Scanlon, D.O.; Bronstein, H.; et al. Hybrid Organic-Inorganic Coordination Complexes as Tunable Optical Response Materials. *Inorg. Chem.* **2016**, *55*, 3393–3400. [CrossRef]
27. Li, Z.; Leed, N.A.; Dickson-Karn, N.M.; Dunbar, K.; Turro, C. Directional charge transfer and highly reducing and oxidizing excited states of new dirhodium(II,II) complexes: Potential applications in solar energy conversion. *Chem. Sci.* **2014**, *5*, 727–737. [CrossRef]
28. Chen, G.-J.; Zhou, Y.; Jin, G.-X.; Dong, Y.-B. [Dy(acac)$_3$(dppn)]·C_2H_5OH: Construction of a single-ion magnet based on the square-antiprism dysprosium(III) ion. *Dalton Trans.* **2014**, *43*, 16659–16665. [CrossRef] [PubMed]
29. Zhang, L.; Yue, S.; Li, B.; Fan, D. A series of [Cu(N-N)(P-P)]BF_4 complexes: Luminescence quenching caused by electron-configuration transformation in excited state. *Inorg. Chim. Acta* **2012**, *384*, 225–232. [CrossRef]
30. Kulmaczewski, R.; Halcrow, M.A. Structures and spin states of crystalline [Fe(NCS)$_2L_2$] and [FeL_3]$^{2+}$ complexes (L = an annelated 1,10-phenanthroline derivative). *CrystEngComm* **2016**, *18*, 2570–2578. [CrossRef]
31. Lin, R.-K.; Chiu, C.-I.; Hsu, C.-H.; Lai, Y.-J.; Venkatesan, P.; Huang, P.-H.; Lai, P.-S.; Lin, C.-C. Photocytotoxic Copper(II) Complexes with Schiff-Base Scaffolds for Photodynamic Therapy. *Chem. Eur. J.* **2018**, *24*, 4111–4120. [CrossRef]
32. Foxon, S.P.; Metcalfe, C.; Adams, H.; Webb, M.; Thomas, J.A. Electrochemical and Photophysical Properties of DNA Metallo-intercalators Containing Ruthenium(II) Tris(1-pyrazolyl)methane Unit. *Inorg. Chem.* **2007**, *46*, 409–416. [CrossRef] [PubMed]
33. Lameijer, L.N.; Breve, T.G.; van Rixel, V.H.S.; Askes, S.H.C.; Siegler, M.A.; Bonnet, S. Effects of the Bidentate Ligand on the Photophysical Properties, Cellular Uptake, and (Photo)cytotoxicity of Glycoconjugates Based on the [Ru(tpy)(NN)(L)]$^{2+}$ Scaffold. *Chem. Eur. J.* **2018**, *24*, 2709–2717. [CrossRef]
34. Scharwitz, M.A.; Ott, I.; Geldmacher, Y.; Gust, R.; Sheldrick, W.S. Cytotoxic half-sandwich rhodium(III) complexes: Polypyridyl ligand influence on their DNA binding properties and cellular uptake. *J. Organomet. Chem.* **2008**, *693*, 2299–2309. [CrossRef]
35. Yam, V.W.-W.; Lo, K.K.-W.; Cheung, K.-K.; Kong, R.Y.-C. Synthesis, photophysical properties and DNA binding studies of novel luminescent rhenium(I) complexes. X-ray crystal structure of [Re(dppn)(CO)$_3$(py)](OTf). *J. Chem. Soc. Chem. Commun.* **1995**, *1995*, 1191–1193. [CrossRef]
36. Hall, J.P.; O'Sullivan, K.; Naseer, A.; Smith, J.A.; Kelly, J.M.; Cardin, C.J. Structure determination of an intercalating ruthenium dipyridophenazine complex which kinks DNA by semiintercalation of a tetraazaphenanthrene ligand. *Proc. Natl. Acad. Sci. USA* **2011**, *108*, 17610–17614. [CrossRef]
37. Song, H.; Kaiser, J.T.; Barton, J.K. Crystal structure of Δ-[Ru(bpy)$_2$dppz]$^{2+}$ bound to mismatched DNA reveals side-by-side metalloinsertion and intercalation. *Nature Chem.* **2012**, *4*, 615–620. [CrossRef] [PubMed]
38. Skórka, Ł.; Filapek, M.; Zur, L.; Małecki, J.G.; Pisarski, W.; Olejnik, M.; Danikiewicz, W.; Krompiec, S. Highly Phosphorescent Cyclometalated Iridium(III) Complexes for Optoelectronic Applications: Fine Tuning of the Emission Wavelength through Ancillary Ligands. *J. Phys. Chem. C* **2016**, *120*, 7284–7294. [CrossRef]
39. Sheldrick, G.M. *SHELXT*—Integrated space-group and crystal-structure determination. *Acta Crystallogr. Sect. A Found. Adv.* **2015**, *71*, 3–8. [CrossRef]
40. Sheldrick, G.M. Crystal structure refinement with *SHELXL*. *Acta Crystallogr. Sect. C Struct. Chem.* **2015**, *71*, 3–8. [CrossRef]